

## Electronic Supplemantary Information

### **Synthesis of the Molecular Amalgam $[\{AuHg_2(o\text{-}C_6F_4)_3\}\{Hg_3(o\text{-}C_6F_4)_3\}]^-$ : a Rare Example of a Heterometallic Homoleptic Metallacycle**

Tania Lasanta, José M. López-de-Luzuriaga,\* Miguel Monge, M. Elena Olmos, and David Pascual

## SUPPORTING INFORMATION

### CONTENTS

Experimental	2
Computational Details	3
Figure S1. Experimental and Simulated ESI(-) spectra of complex <b>1</b> .	4
Table S1. Details of data collection and structure refinement for complex <b>1</b> .	5
Table S2: Selected bond lengths ( $\text{\AA}$ ) and angles ( $^\circ$ ) for complex <b>1</b> .	6
Figure S2: Columnar disposition of complex <b>1</b> .	7
Figure S3: Columnar disposition of complex <b>1</b> (c axis).	8
Figure S4. Superimposed DOSY spectra for complex $\text{NBu}_4[\text{AuHg}_5(o\text{-C}_6\text{F}_4)_6]$ ( <b>2</b> ) (blue) and the $[\text{Hg}_3(o\text{-C}_6\text{F}_4)_3]$ precursor (red).	9
Table S3: Summary of the $^{19}\text{F}$ signals and their corresponding self-diffusion coefficients for complex $\text{NBu}_4[\text{AuHg}_5(o\text{-C}_6\text{F}_4)_6]$ ( <b>2</b> ) and the trinuclear mercury(II) precursor $[\text{Hg}_3(o\text{-C}_6\text{F}_4)_3]$ .	9
Figure S5: Full optimized representation of model <b>1a</b> .	10
Table S4: More representative angles and distances of the theoretical model <b>1a</b> and crystalline structure of <b>1</b> .	10
Figure S5: Interaction distances and the corresponding interaction energy curves at HF and MP2 levels using non relativistic pseudopotentials.	11
Geometries in XYZ format for the <b>1a</b> Model	12
References	13

**General Procedures.** All reactions were carried out under dry and deoxygenated argon atmosphere using Schlenk techniques. Solvents used in the spectroscopic studies were degassed prior to use.  $[\text{Hg}(o\text{-C}_6\text{F}_4)]_3$  was prepared according to literature method.<sup>[1]</sup> **Caution!** Due to the toxicity of mercury compounds extra care was taken to avoid contact with solid, solution, and airborne mercury products.

**Instrumentation:** IR spectra in the 4000-200  $\text{cm}^{-1}$  range were recorded on Nicolet Nexus FT-IR using Nujol mulls between polyethylene sheets. Carbon and hydrogen analyses were carried out with a Perkin-Elmer 240C microanalyzer.  $^{31}\text{P}\{\text{H}\}$ ,  $^1\text{H}$  and  $^{19}\text{F}$  NMR spectra were recorded on a Bruker ARX 300 spectrometer in  $d_6$ -Acetone solutions. Chemical shifts are quoted relative to  $\text{H}_3\text{PO}_4$  85% ( $^{31}\text{P}$  external),  $\text{SiMe}_4$  ( $^1\text{H}$ , external) and  $\text{CFCl}_3$  ( $^{19}\text{F}$ , external).  $^{19}\text{F}$ -DOSY measurements were carried out on an Agilent DD2 500 MHz instrument equipped with a cryoprobe, using  $d_6$ -Acetone as solvent. Molar conductivity measurements were carried out with a digital Jenway 4010 instrument.

**Synthesis of  $[\text{Au}(\text{PMe}_3)_2]\{\text{AuHg}_2(o\text{-C}_6\text{F}_4)_3\}\{\text{Hg}(o\text{-C}_6\text{F}_4)\}_3$  (1):** To a solution of  $[\text{Hg}(o\text{-C}_6\text{F}_4)]_3$  (0.237 g, 0.227 mmol) in  $\text{CH}_2\text{Cl}_2$  (30 mL) was added two equivalents of  $[\text{Au}(\text{C}_6\text{F}_5)(\text{PMe}_3)]$  (0.200 g, 0.454 mmol). A white suspension appears, and after stirring the mixture for 1 hour complex **1** was isolated by filtration as a white solid. Yield: 77%;  $^1\text{H}$  NMR (300 MHz,  $d_6$ -Acetone):  $\delta = 1.54$  ppm (s);  $^{19}\text{F}$  NMR (283 MHz,  $d_6$ -Acetone):  $\delta = 120.5$  (m,  $^3J_{\text{F-Hg}} = 455$  Hz 6F,  $F_o$ ,  $[\text{Hg}(o\text{-C}_6\text{F}_4)]_3$ ), -158.9 (m, 6F,  $F_m$ ,  $[\text{Hg}(o\text{-C}_6\text{F}_4)]_3$ ), -116.6 (m, 2F,  $F_o$ ,  $(\text{Au}(o\text{-C}_6\text{F}_4))$ ), -122.6 (m,  $^3J_{\text{F-Hg}} = 492$  Hz 2F,  $F_o$ ,  $(\text{Hg}(o\text{-C}_6\text{F}_4))$ ), -125.6 (m,  $^3J_{\text{F-Hg}} = 480$  Hz 2F,  $F_o$ ,  $(\text{Hg}(o\text{-C}_6\text{F}_4))$ ), -160.0 (m, 2F,  $F_m$ ,  $(\text{Hg}(o\text{-C}_6\text{F}_4))$ ), -160.2 (m, 2F,  $F_m$ ,  $(\text{Hg}(o\text{-C}_6\text{F}_4))$ ), -163.7 ppm (m, 2F,  $F_m$ ,  $(\text{Au}(o\text{-C}_6\text{F}_4))$ );  $^{31}\text{P}\{\text{H}\}$  NMR (121.5 MHz,  $d_6$ -Acetone):  $\delta = 7.3$  ppm (s); FT-IR (Nujol mull):  $\nu$  ( $\text{C}_6\text{F}_4$ ) = 1376, 1293, 1078 and 623  $\text{cm}^{-1}$ ; elemental analysis calcd. (%) for  $\text{C}_{42}\text{H}_{18}\text{Au}_2\text{F}_{24}\text{Hg}_5\text{P}_2$ : C 20.70, H 0.74; found: C 20.70, H 0.77. MS (ES+): m/z 349.06  $[\text{Au}(\text{PMe}_3)_2]^+$ ; (ES-): 2087.78  $[\{\text{AuHg}_2(o\text{-C}_6\text{F}_4)_3\}\{\text{Hg}(o\text{-C}_6\text{F}_4)\}_3]^-$ ;  $\Lambda_M$  (acetone) = 142.4  $\Omega^{-1}\cdot\text{cm}^2\cdot\text{mol}^{-1}$ .

**Synthesis of  $\text{NBu}_4[\{\text{AuHg}_2(o\text{-C}_6\text{F}_4)_3\}\{\text{Hg}(o\text{-C}_6\text{F}_4)\}_3]$  (2):** To a solution of  $[\text{Hg}(o\text{-C}_6\text{F}_4)]_3$  (0.314 g, 0.3 mmol) in  $\text{CH}_2\text{Cl}_2$  (30 mL) was added  $\text{NBu}_4[\text{Au}(\text{C}_6\text{F}_5)_2]$  (0.116 g, 0.15 mmol). A white suspension appears, and after stirring the mixture for 1 hour complex **2** was isolated by filtration as a white solid. Yield: 80%;  $^1\text{H}$  NMR (300 MHz,  $d_6$ -Acetone):  $\delta = 0.99$  (t,  $^3J_{\text{H-H}} = 7$  Hz 3H), 1.45 (m), 1.84 (m), 3.46 ppm (m);  $^{19}\text{F}$  NMR (283 MHz,  $d_6$ -Acetone):  $\delta = 120.6$  (m,  $^3J_{\text{F-Hg}} = 461$  Hz 6F,  $F_o$ ,  $[\text{Hg}(o\text{-C}_6\text{F}_4)]_3$ ), -159.1 (m, 6F,  $F_m$ ,  $[\text{Hg}(o\text{-C}_6\text{F}_4)]_3$ ), -116.8 (m, 2F,  $F_o$ ,  $(\text{Au}(o\text{-C}_6\text{F}_4))$ ), -122.6 (m,  $^3J_{\text{F-Hg}} = 488$  Hz 2F,  $F_o$ ,  $(\text{Hg}(o\text{-C}_6\text{F}_4))$ ), -125.8 (m,  $^3J_{\text{F-Hg}} = 489$  Hz 2F,  $F_o$ ,  $(\text{Hg}(o\text{-C}_6\text{F}_4))$ ), -159.6 (m, 2F,  $F_m$ ,  $(\text{Hg}(o\text{-C}_6\text{F}_4))$ ), -160.4 (m, 2F,  $F_m$ ,  $(\text{Hg}(o\text{-C}_6\text{F}_4))$ ), -164.0 ppm (m, 2F,  $F_m$ ,  $(\text{Au}(o\text{-C}_6\text{F}_4))$ ); FT-IR (Nujol mull):  $\nu$  ( $\text{C}_6\text{F}_4$ ) = 1378, 1301, 1078 and 1008  $\text{cm}^{-1}$ ; elemental analysis calcd. (%) for  $\text{C}_{52}\text{H}_{36}\text{AuF}_{24}\text{Hg}_5\text{N}$ : C 26.80, H 1.56, N 0.60; found: C 26.72, H 1.58, N 0.63. MS (ES+): m/z 246.32  $[\text{NBu}_4]^+$ ; (ES-): 2087.78  $[\{\text{AuHg}_2(o\text{-C}_6\text{F}_4)_3\}\{\text{Hg}(o\text{-C}_6\text{F}_4)\}_3]^-$ ;  $\Lambda_M$  (acetone) = 151.6  $\Omega^{-1}\cdot\text{cm}^2\cdot\text{mol}^{-1}$ .

**Crystallography.** Crystal Structure Analysis.  $\text{C}_{42}\text{H}_{18}\text{Au}_2\text{F}_{24}\text{Hg}_5\text{P}_2$ , Mr=2437.39, 0.45x0.05x0.05 mm, monoclinic,  $C2/c$ ,  $a=22.8022(12)$ ,  $b=16.7195(9)$ ,  $c=13.2363(4)$  Å,  $b=108.23(1)$ ,  $V=4792.9(4)$  Å<sup>3</sup>,  $Z=4$ ,  $r_{\text{calcd}}=3.378$  gcm<sup>-3</sup>,  $m=22.245$  mm<sup>-1</sup>, Mo Ka radiation,  $\lambda=0.71073$  Å,  $T=-153$  °C,  $2q_{\text{max}}=55^\circ$ , 36348 measured and 5469 observed

reflections,  $R_{int}=0.0927$ ,  $R1=0.0858$ ,  $wR2=0.1976$ , maximum residual electron density=2.378 e·Å<sup>3</sup>. The crystals were mounted in inert oil on glass fibers and transferred to the cold gas stream of a Nonius Kappa CCD diffractometer equipped with an Oxford Instruments low-temperature attachment. Scan type w and f. Absorption correction: numerical (based on multiple scans). The structure was solved by direct methods and refined on  $F^2$  using the program SHELXL-97.{Sheldrick:1997wg} All non-hydrogen atoms were anisotropically refined. Hydrogen atoms were included using a riding model. As the asymmetric unit contains only half a molecule, the metal atom within the trinuclear [Hg<sub>2</sub>M(C<sub>6</sub>F<sub>4</sub>)<sub>3</sub>] unit that maintains the short metallophilic interaction was refined as gold or mercury with occupancies of 50% for each one. The residual electron density is due to the high absorption coefficient related to presence of seven heavy metal atoms. CDC-1429227 contains the supplementary crystallographic data for this paper. These data can be obtained free of charge via [www.ccdc.cam.ac.uk/conts/retrieving.html](http://www.ccdc.cam.ac.uk/conts/retrieving.html) (or from the Cambridge Crystallographic Data Centre, 12 Union Road, Cambridge CB2 1EZ, UK; fax: (+44) 1223-336-033; or e-mail: [deposit@ccdc.cam.ac.uk](mailto:deposit@ccdc.cam.ac.uk)).

**Computational details.** All calculations were performed using the Gaussian 09 suite of programs<sup>[2]</sup> using Hartree-Fock (HF) and MP2<sup>[4,5]</sup> levels of theory. The interaction energy between metal fragments at Hartree-Fock (HF) and MP2 levels of theory was obtained according to equation:

$$\Delta E = E_{AB}^{(AB)} - E_A^{(AB)} - E_B^{(AB)} = V(R)$$

A counterpoise correction for the basis-set superposition error (BSSE)<sup>[6]</sup> on  $\Delta E$  was thereby performed. We fitted the calculated points using a four-parameter equation, which had been previously used<sup>[7]</sup> to derive the Herschbach-Laurie relation:

$$\Delta E = V(R) = Ae^{-BR} - CR^{-\eta}$$

We carried out first the full optimization of model **1a**, which displays the same arrangement to that found experimentally in the X-ray structural analysis. Since the interaction between the trinuclear fragments include several types of interactions (i.e. Au(I)…Hg(II), C<sub>ipso</sub>…Hg and Hg(II)…Hg(II)) we tried to compute the isolated Au(I)…Hg(II) interaction energy in other model systems by turning one of the trinuclear fragments out of the interaction region. Unfortunately, other repulsive interactions appeared at the same time, what made impossible this analysis.

**Basis Sets.** The 19-valence electron (VE) quasirelativistic (QR) pseudopotential (PP) was employed for gold<sup>[8]</sup> together with two f-type polarization functions.<sup>[9]</sup> Similarly, the 20-valence valence electron (VE) quasirelativistic (QR) pseudopotential (PP) of Andrae<sup>[8]</sup> was employed for mercury together with two f-type polarization functions.<sup>[10]</sup> The atoms P, and C were treated by Stuttgart pseudopotentials,<sup>[11]</sup> including only the valence electrons for each atom. For these atoms double-zeta basis sets of ref 10 were used, augmented by d-type polarization functions.<sup>[12-14]</sup> For the H atom, a double-zeta, plus a p-type polarization function was used.<sup>[3,15]</sup>

Parámetros de adquisición  
Tipo de Fuente y polaridad: ESI Negative

-MS, 0.24-0.37 min #(14-22)

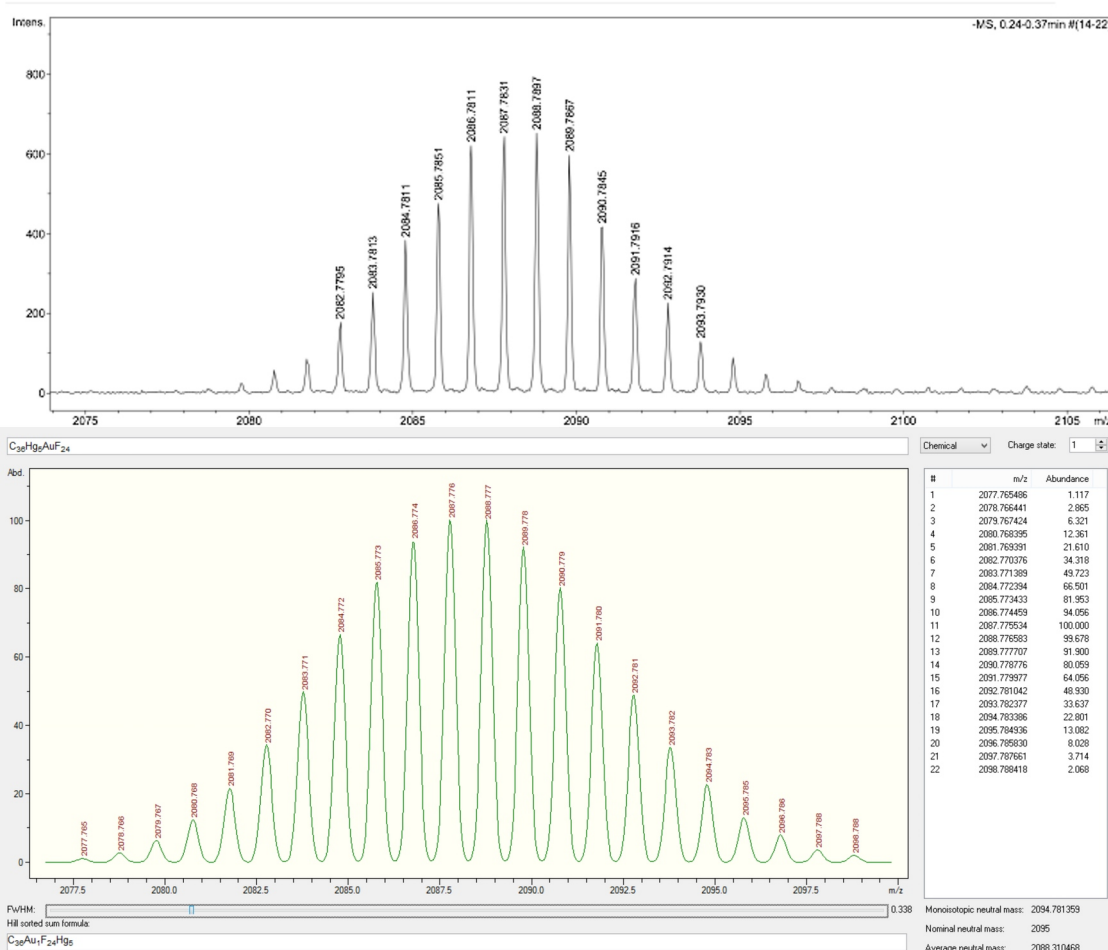


**Figure S1:** Experimental ESI(-) spectrum of complex 1 (top), and their simulation (down).

**Table S1:** Details of data collection and structure refinement for complex **1**.

Empirical formula	C42 H18 Au2 F24 Hg5 P2
Formula weight	2437.39
Temperature	120(2) K
Wavelength	0.71073 Å
Crystal system	Monoclinic
Space group	C2/c
Unit cell dimensions	$a = 22.8022(12)$ Å $\alpha = 90^\circ$ $b = 16.7195(9)$ Å $\beta = 108.232(3)^\circ$ $c = 13.2363(4)$ Å $\gamma = 90^\circ$
Volume	4792.9(4) Å <sup>3</sup>
Z	4
Density (calculated)	3.378 Mg/m <sup>3</sup>
Absorption coefficient	22.245 mm <sup>-1</sup>
F(000)	4296
Crystal size	0.45 x 0.05 x 0.05 mm <sup>3</sup>
Theta range for data collection	1.54 to 27.45°
Index ranges	-29<=h<=29, -21<=k<=21, -16<=l<=16
Reflections collected	36348
Independent reflections	5469 [R(int) = 0.0927]
Completeness to theta = 27.45°	99.5 %
Refinement method	Full-matrix least-squares on F <sup>2</sup>
Data / restraints / parameters	5469 / 108 / 330
Goodness-of-fit on F <sup>2</sup>	1.403
Final R indices [I>2sigma(I)]	R1 = 0.0859, wR2 = 0.1928
R indices (all data)	R1 = 0.1013, wR2 = 0.1977
Largest diff. peak and hole	2.414 and -3.535 e.Å <sup>-3</sup>

**Table S2:** Selected bond lengths ( $\text{\AA}$ ) and angles ( $^\circ$ ) for complex **1**.

Hg(3)-Au(3)#2	3.097(2)
Hg(1)-C(1)	2.11(3)
Hg(1)-C(26)	2.11(3)
Hg(2)-C(6)	2.06(3)
Hg(2)-C(11)	2.12(3)
Hg(3)-C(16)	2.07(3)
Hg(3)-C(21)	2.05(3)
Au(3)#2-C(16)#2	2.07(3)
Au(3)#2-C(21)#2	2.05(3)
Au(1)-P	2.302(7)
Hg(1)-Au(3)#1	3.3613(14)
Hg(3)-Hg(1)#1	3.3613(14)
Hg(2)-C(11)#2	3.236(27)
Hg(2)-C(22)#1	3.243(28)
C(26)-Hg(1)-C(1)	175.7(11)
C(6)-Hg(2)-C(11)	178.5(12)
C(21)-Hg(3)-C(16)	175.7(11)
C(21)#2-Au(3)#2-C(16)#2	175.7(11)
P-Au(1)-P#3	171.4(4)
Hg(3)#2-Hg(3)-Hg(1)#1	173.33(5)
Hg(3)#2-Au(3)-Hg(1)#1	173.33(5)

---

Symmetry transformations used to generate equivalent atoms:

#1 -x,-y+2,-z #2 -x,y,-z+1/2 #3 -x+1,y,-z+1/2

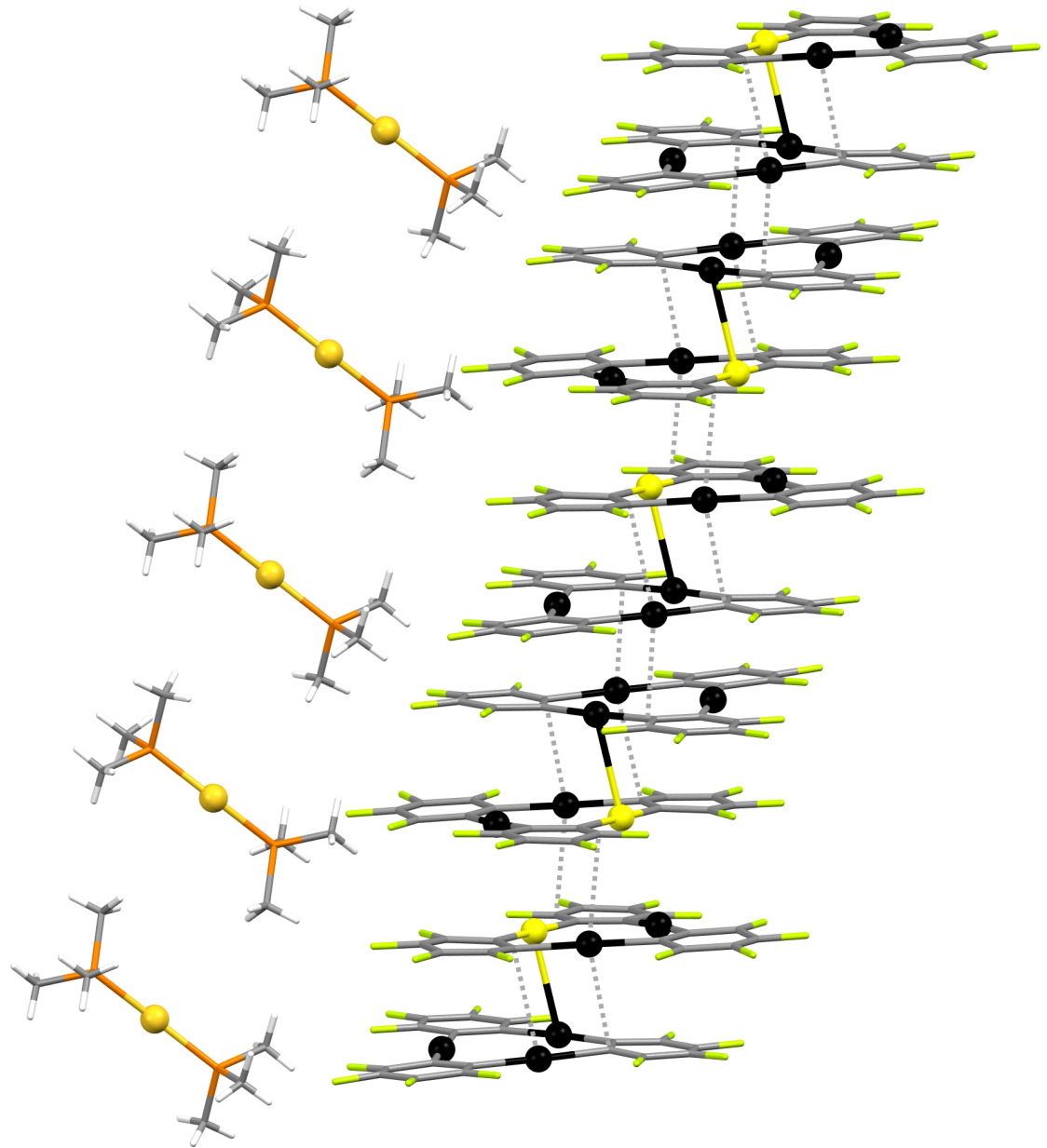


**Figure S2:** Columnar disposition of complex **1**.

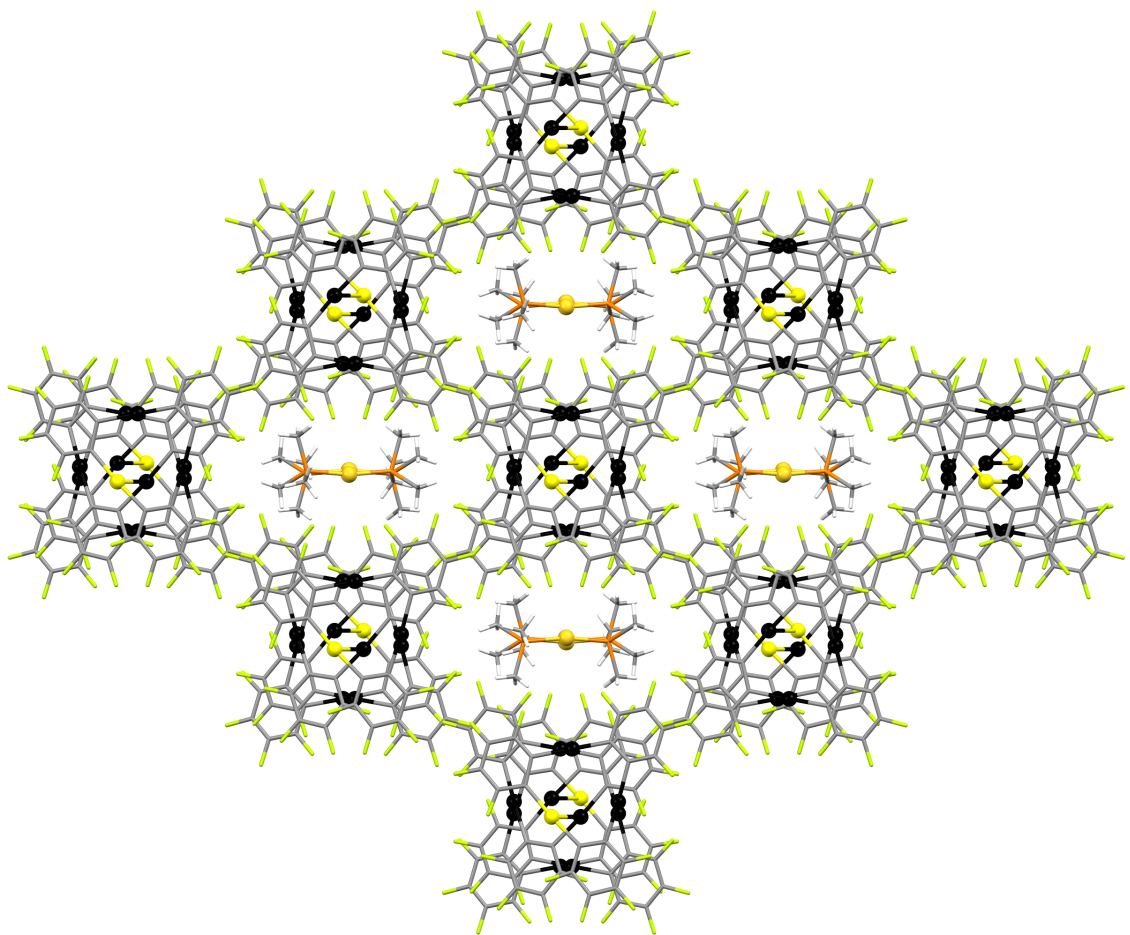


**Figure S3:** Columnar disposition of the molecules along the crystallographic *c* axis.

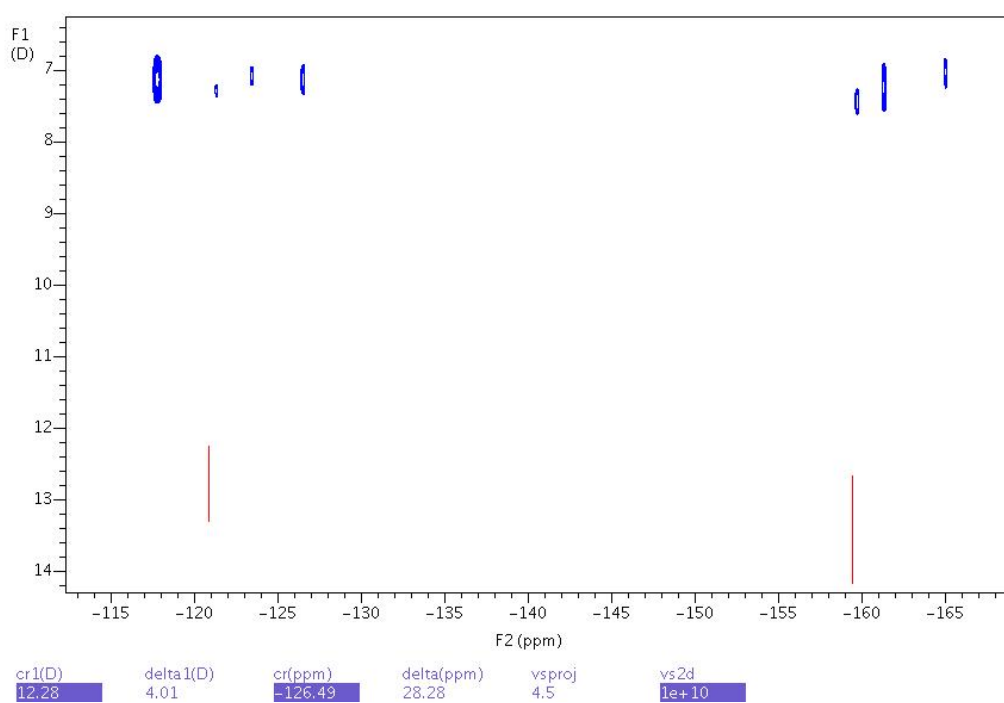


**Figure S4:** Superimposed DOSY spectra for complex NBu<sub>4</sub>[AuHg<sub>5</sub>(o-C<sub>6</sub>F<sub>4</sub>)<sub>6</sub>] (**2**) (blue) and the [Hg<sub>3</sub>(o-C<sub>6</sub>F<sub>4</sub>)<sub>3</sub>] precursor (red).

**Table S3:** Summary of the <sup>19</sup>F signals and their corresponding self-diffusion coefficients for complex NBu<sub>4</sub>[AuHg<sub>5</sub>(o-C<sub>6</sub>F<sub>4</sub>)<sub>6</sub>] (**2**) and the trinuclear mercury(II) precursor [Hg<sub>3</sub>(o-C<sub>6</sub>F<sub>4</sub>)<sub>3</sub>].

#### NBu<sub>4</sub>[AuHg<sub>5</sub>(o-C<sub>6</sub>F<sub>4</sub>)<sub>6</sub>] (**2**)

Peak	Freq/ppm	Amplitude	D <sub>t</sub> /(10e-10 m <sup>2</sup> /s)+/-std.err.
1	-117.8353	0.0019	7.3037 ± 0.200554
2	-121.4332	0.0145	7.3336 ± 0.025698
3	-123.4467	0.0050	6.9920 ± 0.056305
4	-126.6485	0.0039	7.1981 ± 0.099395
5	-159.8550	0.0135	7.3568 ± 0.058087
6	-161.5055	0.0037	7.2721 ± 0.191469
7	-165.1034	0.0039	6.8318 ± 0.078790

#### [Hg<sub>3</sub>(o-C<sub>6</sub>F<sub>4</sub>)<sub>3</sub>]

Peak	Freq/ppm	Amplitude	D <sub>t</sub> /(10e-10 m <sup>2</sup> /s)+/-std.err.
1	-120.9435	0.5590	13.4020 ± 0.101135
2	-159.3772	0.6506	13.6884 ± 0.164505

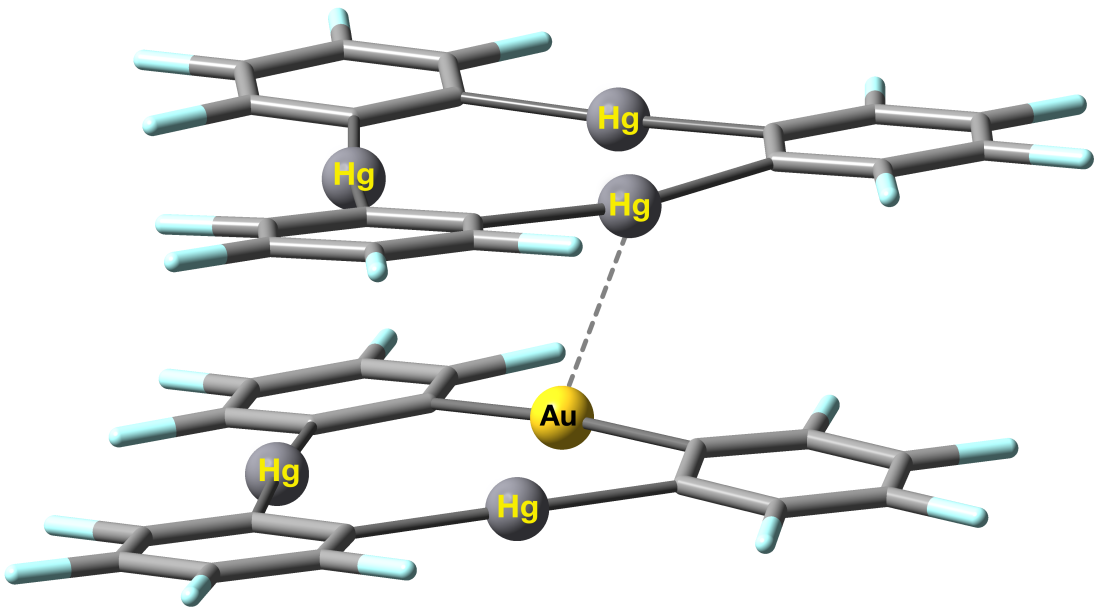


**Figure S5:** Full optimized representation of model **1a**.

**Table S4:** More representative angles and distances of the theoretical model **1a** and crystalline structure of **1**.

	Hg-Au (Å)	Au-C (Å)	C-Au-C (°)	Hg-C (Å)	C-Hg-C (°)
X-Ray	3.10	2.05, 2.07	175.4	2.05-2.10	175.7-178.9
Model <b>1a</b>	3.20	2.06, 2.07	174.6	2.09-2.12	170.6-175.8

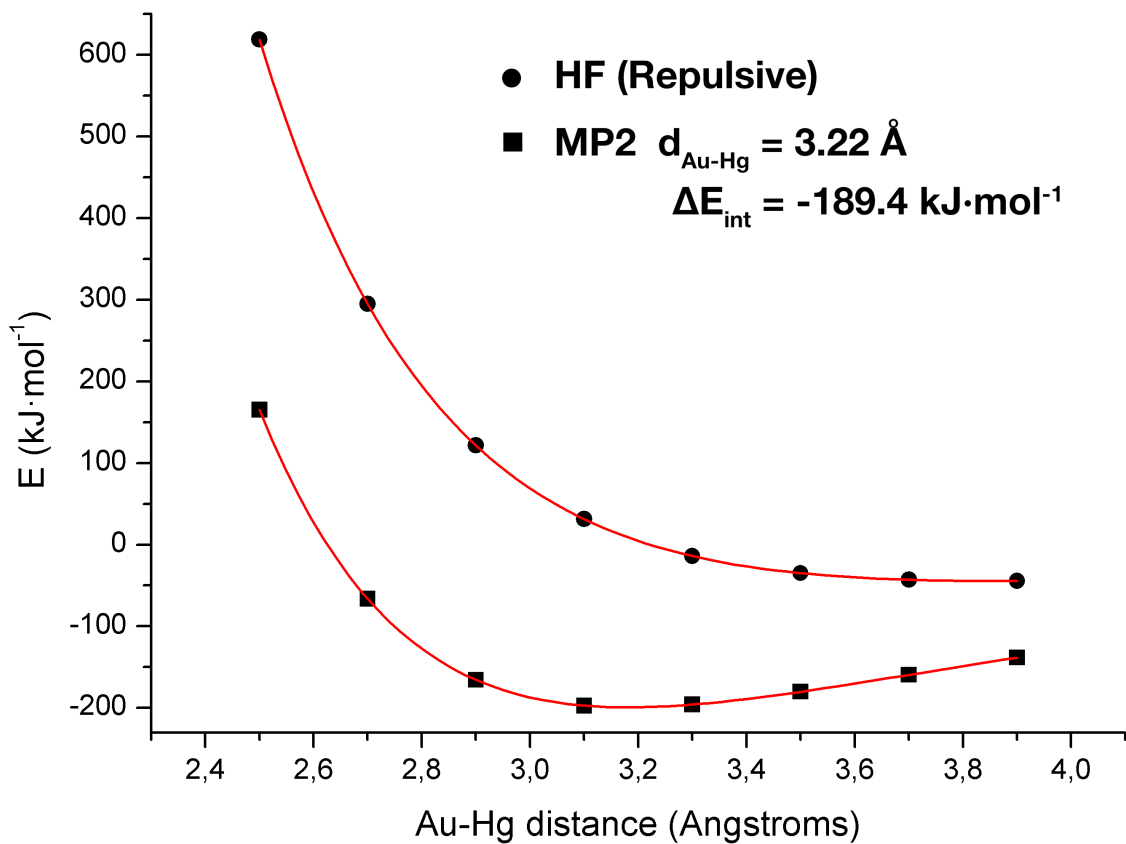


**Figure S5:** Interaction distances and the corresponding interaction energy curves at HF and MP2 levels using non relativistic pseudopotentials.

## GEOMETRIES IN XYZ FORMAT FOR THE 1a MODEL

Hg	0.00000000	0.00000000	0.00000000
Hg	0.00000000	0.00000000	3.67558559
F	5.43855388	0.00000000	-0.33219268
F	-5.34799706	0.33960866	0.48835579
F	-3.03103400	0.21320022	-0.86624887
F	3.11624040	-0.10505457	-4.38785601
F	-3.02176700	0.25454677	4.54173769
C	1.86153021	-0.01123043	-0.97384632
C	4.29842161	-0.04297560	-2.36144985
C	3.10197149	-0.06470675	-3.06359353
C	-2.98133323	0.25847859	3.20400815
C	1.90685638	-0.04272436	-2.35730283
C	-1.76829673	0.18822650	2.54199398
C	4.26272699	-0.00142286	-0.97364769
C	-1.77045414	0.17112266	1.12939940
C	-4.19725961	0.31034720	2.53230432
C	3.07828909	0.00864616	-0.25854361
C	-4.19956384	0.29747706	1.14539889
F	5.44716067	-0.06624217	-3.01763418
F	-5.34271395	0.36146222	3.19276643
F	0.77362253	-0.06163670	-3.07021146
C	-2.98646144	0.23145710	0.47065978
Hg	3.16550096	-0.10433638	1.85179092
C	1.86553601	0.07982152	4.67418409
C	3.08997875	0.08664260	3.96442260
F	5.44432985	0.25630277	4.05359924
F	0.76459049	0.19291746	6.75981491
C	3.08611365	0.34915181	6.76332583
C	4.26410411	0.24381383	4.68370695
C	4.28583490	0.36823559	6.06897235
C	1.90023388	0.21795926	6.05186011
F	3.08763197	0.42406305	8.08372166
F	5.42606187	0.46936263	6.72992057
Hg	4.32157959	-3.07366235	4.37735487
Hg	0.81624986	-3.07537672	5.50072067
F	2.92506597	-3.09024910	-0.83997770
F	5.48459417	-2.89236015	9.62498435
F	6.06514427	-2.97922063	7.00536220
F	7.49889954	-3.44518035	0.01079769
F	0.91690798	-3.06225043	8.65777503
C	4.71115037	-3.11323726	2.32322054
C	5.19487751	-3.27511199	-0.41801331
C	6.26065130	-3.32925079	0.47026398
C	2.17646719	-3.05198461	8.20787316
C	5.99772866	-3.25620351	1.83067959
C	2.43434919	-3.09719231	6.84733980
C	3.90155687	-3.14471870	0.07065995
C	3.78013820	-3.07700292	6.41389198
C	3.18762646	-2.98398715	9.15785800
C	3.61234752	-3.04509375	1.42840843
C	4.50815761	-2.96186297	8.73355271
F	5.42805769	-3.32521605	-1.72246255
F	2.91132836	-2.93521505	10.45186749
F	7.04181416	-3.32584699	2.66645281
C	4.77898366	-3.01090537	7.37185999
Au	1.64789318	-2.91350461	2.05421615
C	-0.69281513	-3.04285328	4.04601129
C	-0.31316760	-2.97513791	2.67815534
F	-1.07172976	-2.94417974	0.43186961
F	-2.40254577	-3.18840301	5.67399380
C	-3.03744254	-3.15416152	3.43296278
C	-1.33976000	-3.02205384	1.74423324
C	-2.68095167	-3.10487992	2.09181478
C	-2.03286078	-3.13073488	4.39023784
F	-4.31706477	-3.20796866	3.77312482
F	-3.62942611	-3.10381247	1.16681932

## References

- [1] P. Sartori, A. Golloch, *Chem. Ber.* **1968**, *101*, 2004–2009.
- [2] M. J. Frisch, G. W. Trucks, H. B. Schlegel, G. E. Scuseria, M. A. Robb, J. R. Cheeseman, G. Scalmani, V. Barone, B. Mennucci, G. A. Petersson, et al., **2009**.
- [3] G. M. Sheldrick, *SHELX-97, Program for Crystal Structure Refinement*, University of Göttingen, Göttingen, **1997**.
- [4] C. Møller, M. S. Plesset, *Phys. Rev.* **1934**, *46*, 618–622.
- [5] W. J. Hehre, L. Radom, P. V. R. Schleyer, J. A. Pople, *Ab Initio Molecular Orbital Theory*, John Wiley, New York, **1986**.
- [6] S. F. Boys, F. Bernardi, *Mol. Phys.* **1970**, *19*, 553–566.
- [7] D. R. Herschbach, V. W. Laurie, *J. Chem. Phys.* **1961**, *35*, 458.
- [8] D. Andrae, U. Häußermann, M. Dolg, H. Stoll, H. Preuss, *Theor. Chim. Acta* **1990**, *77*, 123–141.
- [9] P. Pyykkö, N. Runeberg, F. Mendizabal, *Chem. Eur. J.* **1997**, *3*, 1451–1457.
- [10] J. M. L. Martin, A. Sundermann, *J. Chem. Phys.* **2001**, *114*, 3408–3420.
- [11] A. Bergner, M. Dolg, W. Küchle, H. Stoll, H. Preuss, *Mol. Phys.* **1993**, *80*, 1431.
- [12] R. Usón, A. Laguna, M. Laguna, J. Jiménez, M. P. Gómez, A. Sainz, P. G. Jones, *J. Chem. Soc., Dalton Trans.* **1990**, 3457–3463.
- [13] S. Huzinaga, J. Andzelm, *Gaussian Basis Sets for Molecular Orbital Calculations*, Elsevier, Amsterdam, **1984**.
- [14] M. A. Bennett, M. Contel, D. C. R. Hockless, L. L. Welling, *Chem. Commun.* **1998**, *21*, 2401–2402.
- [15] S. Huzinaga, *J. Chem. Phys.* **1965**, *42*, 1293–1302.